



HAL
open science

ALINE: A device dedicated to understanding radio-frequency sheaths

S. Devaux, E. Faudot, Jérôme Moritz, S. Heuraux

► **To cite this version:**

S. Devaux, E. Faudot, Jérôme Moritz, S. Heuraux. ALINE: A device dedicated to understanding radio-frequency sheaths. Nuclear Materials and Energy, 2017, 12, pp.908-912. 10.1016/j.nme.2017.07.003 . hal-03545106

HAL Id: hal-03545106

<https://hal.science/hal-03545106>

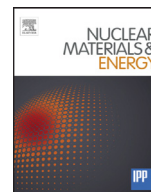
Submitted on 27 Jan 2022

HAL is a multi-disciplinary open access archive for the deposit and dissemination of scientific research documents, whether they are published or not. The documents may come from teaching and research institutions in France or abroad, or from public or private research centers.

L'archive ouverte pluridisciplinaire **HAL**, est destinée au dépôt et à la diffusion de documents scientifiques de niveau recherche, publiés ou non, émanant des établissements d'enseignement et de recherche français ou étrangers, des laboratoires publics ou privés.



Distributed under a Creative Commons Attribution - NonCommercial - NoDerivatives 4.0
International License



ALINE: A device dedicated to understanding radio-frequency sheaths



S. Devaux*, E. Faudot, J. Moritz, S. Heuraux

Institut Jean Lamour, UMR 7198 CNRS, Université de Lorraine, 54500 Vandoeuvre les Nancy, France

ARTICLE INFO

Article history:

Received 30 June 2016

Revised 29 May 2017

Accepted 8 July 2017

Available online 24 July 2017

Keywords:

Magnetized plasma

Sheath

Langmuir probe

Radio-Frequency

ABSTRACT

In fusion devices, radiofrequency (RF) antennas are used for heating the plasma. Those antennas and the plasma interact with each other through the so-called RF sheaths, layers of plasma where the quasi-neutrality breaks down and large electric fields arise. Among the effects of RF sheaths, there is the enhancement of the particles and energy fluxes toward the surface of the antenna, which in turn generate hot spots and release impurities, which are both deleterious for plasma operations. RF sheaths comprehension stumbles on the difficulty to achieve in situ measurements of the sheath properties, as scrape-off layer plasmas are a harsh environment. The very goal of the ALINE device is to tackle this issue and to fulfil the blank between numerical simulations and full-scale experiment by providing measurements within the RF sheaths in a controlled environment. In this paper we report on the latest experimental results from ALINE, in which a cylindrical Langmuir probe mounted on a remotely controlled and programmable arm allows for plasma characterizations in the three dimensions of space around the stainless steel antenna, including the sheath. We present a series of density and potential profiles and three dimension (3D) maps in the plasma surrounding a stainless-steel RF antenna as well as in the sheath itself, for unmagnetized and magnetized plasmas.

© 2017 The Authors. Published by Elsevier Ltd.
This is an open access article under the CC BY-NC-ND license.
(<http://creativecommons.org/licenses/by-nc-nd/4.0/>)

Introduction

Sheaths are commonly observed in almost all man made plasmas as they arise as soon as a surface is in contact with a plasma. No matter if the surface belongs to the confining vessel, the device probing the plasma or the cathode generating it, a transition layer appears and shields the plasma from the surface. This so-called Debye sheath is the region where quasineutrality breaks down and where large electric fields arise. Depending on the wall bias and the electric charge of the particles, the effect of the sheath is to repel or accelerate those particles. The entrance of the sheath is the point where the ions speed exceeds the sound one, satisfying the so-called Bohm criterion. Sheaths have been studied for many years by different methods (experiments, numerical simulations and theory) but still are a very active research field in plasma physics and in fusion in particular, for they govern the plasma-interactions which may have a dramatic impact on the plasma facing components. The situation in fusion devices (tokamaks and stellarators) is complicated by the presence of a magnetic field on the wall, which leads to the existence of an inter-

mediate region known as magnetic pre-sheath [1]. Moreover, non-steady sheaths such as radio-frequency sheaths, i.e. sheaths that respond to a varying wall potential (imposed by an external generator), can transform a null time-average electric field into one accelerating even more the ions toward the wall [2,3]. This phenomenon known as potential rectification is of paramount importance for Ion Cyclotron Resonance Heating (ICRH) antenna where they generate hot spots on the frame those antennae and enhanced the sputtering of their surface as well as the release of impurities into the plasma. In this paper we present the ALINE device which has been built and developed with the very goal of experimentally studying RF sheaths in nearly ideal conditions, i.e. a very good accessibility of the plasma and sheath for various diagnostics, so that all the different properties of the plasma species can be accurately measured. We here first provide an overview of the available diagnostics. We then focus 3D maps of the plasma floating potential and ion density for both a magnetized and unmagnetized plasma. We conclude this paper with the foreseen developments of our capabilities.

The ALINE device

The ALINE device [4] is A LINEar cylindrical device (Fig. 1a) of 100 cm by 30 cm in which low pressure plasma of either Argon,

* Corresponding author.

E-mail address: stephane.devau@univ-lorraine.fr (S. Devaux).

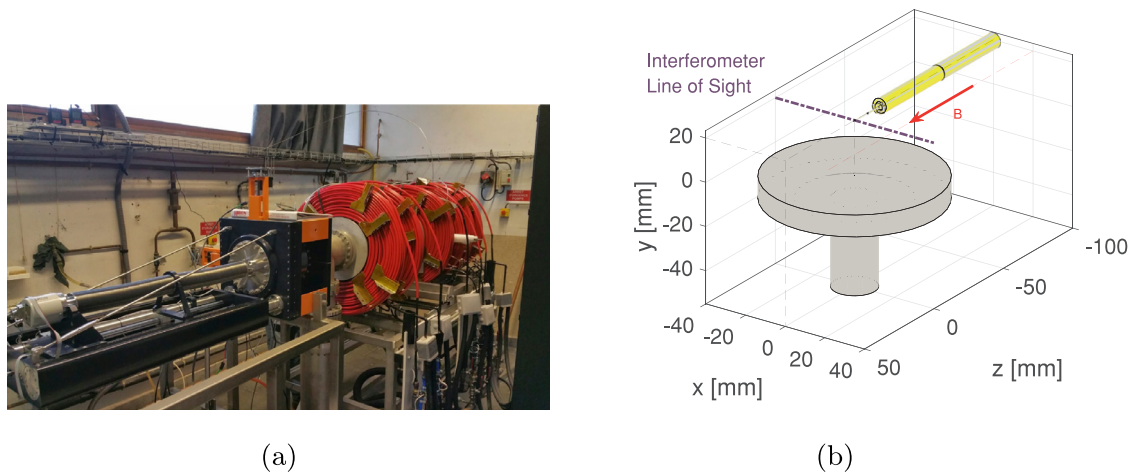


Fig. 1. (a) The cylindrical chamber of The ALINE device and its 6 copper coils (red) that can create a magnetic field up to 0.1 T. (b) Schematic of the experiment. The surface of the RF antenna is located at $(x, y, z) = (0, -10, 0)$ mm. The magnetic field (red arrow) is along the z direction. The probe (yellow) moves in the three direction. (For interpretation of the references to color in this figure legend, the reader is referred to the web version of this article.)

Helium or Hydrogen can be produced with typical neutral pressure of $10^{-2} - 10^{-3}$ m bar. An external magnetic field parallel to the axis of the cylinder and to the antenna can be applied thanks to 6 copper coils powered by 3 independent generators delivering up to 250 A. The resulting magnetic field is fairly homogeneous along the axis of the chamber [4] and can reach up to 0.1 T, leading to a Larmor radius of ≈ 1 mm for Argon ions at the room temperature. The plasma itself is produced by a RF antenna (on which a blocking capacitor in series is installed) that operates between 10 kHz and 250 MHz and delivers up to 600 W of input power. The vacuum in the vessel is maintained by two different pumping systems, a butterfly valve and a turbo-pump that insure a remaining background pressure below 10^{-7} mbar. The different plasmas studied in ALINE and presented in this paper are obtained with a neutral pressure between 10^{-4} and 10^{-2} mbar. Typical plasmas in ALINE have a density in the $10^{14} - 10^{17}$ m³ range with an electron temperature of 1 – 6 eV, giving a Debye length ranging from 1 mm to 0.01 mm. Stability and reproducibility of plasmas are continuously checked by the repetition of a reference plasma, which also insures that the diagnostics are still working as expected. Typically, one needs to wait for 20 min after a modification of an input parameters for the plasma to be stabilized, after what the plasma remains steady for several hours without noticeable variation of its density and temperature.

Plasma diagnostics

The main interest of the ALINE device for studying sheath physics relies on its diagnostics for probing the plasma. Indeed, the vessel is equipped with 14 ports available for plasma diagnostics. The main diagnostic is a RF-compensated Langmuir probe [5] made of tungsten cylindrical tip of 10 mm by 0.15 mm in diameter that can be biased from -200 V to 100 V. The time needed to record one IV characteristic is about 10^{-3} s, and each measurement is averaged over 20 ramp of voltage, much longer than the duration of a RF period: $\approx 10^{-8}$ s at 35 MHz. A typical IV characteristic measured in ALINE can be found in [4]. The probe is mounted on a remote manipulator system translatable in the three directions of space around the antenna. The manipulator is actuated by three step motors which can position the probe with an accuracy of 0.1 mm, which is of the same order as the probe width. It has to be noted that the accuracy is not limited by the step motors with the accuracy of 5×10^5 mm, but by the current determina-

tion of the reference position, a mechanical limit switch. The manipulator is controlled by a software that also controls and synchronizes the different other diagnostics so that 3D maps of typically 3000–4000 points can be automatically performed with periodic checks of the input parameters. Plasma density measurements derived from the probe characteristics are cross-checked thanks to the use of microwave interferometer delivering electromagnetic wave at 26.5 GHz (40 mW) providing line integrated measurement of the electron density. The working densities of the interferometer (i.e. densities for which the wave can propagate into the plasma) spread from 10^{15} to 10^{18} m³. The emitter and receiver of the device are installed so that the measured line goes through the vessel 50 mm above the surface of the antenna at $z = 0$, along the x direction (see Fig. 1b). A numeric oscilloscope monitors the input and reflected powers of the antenna, as well as its surface polarization. The ALINE equipment is completed with a high definition (HD) webcam that allows for visual investigations of the plasma and measurement of the sheath width. All the data recorded are automatically stored into a database together with the experimental parameters.

3D maps in an unmagnetized plasma

In the previous section, the main diagnostic on ALINE, a Langmuir probe that can be moved around the antenna, has been described. From its current-voltage characteristics, one can derive the floating and plasma potentials and, with a proper model [6,7], ion and electron densities, as well as the electron temperature. In this section we present 3D maps for such measurements performed in a RF plasma with 30 W of power injected at a frequency of 30 MHz, in an Argon plasma with neutral pressure of 5.9×10^3 mbar. Each map is made of 3032 measurement points, recorded every 10 mm on $9 \times 9 \times 46$ (x,y,z) matrix, for a total of 5 h of experiment. On Figs. 2a and b such a map is presented for the floating potential and the ion density, respectively. The first observation from Fig. 2a is that the floating potential is rather uniform in the entire chamber at a value of $40.5 \text{ V} \pm 2.6 \text{ V}$, to be compared to the plasma potential (not presented here and as uniform as the floating potential) of $49.2 \text{ V} \pm 3.6 \text{ V}$ measured respectively to the grounded chamber. The average electron temperature measured by the probe of $T_e = 1.97 \text{ eV}$ is coherent with the 1.89 eV derived from the difference between the plasma potential V_{Plasma} and the floating

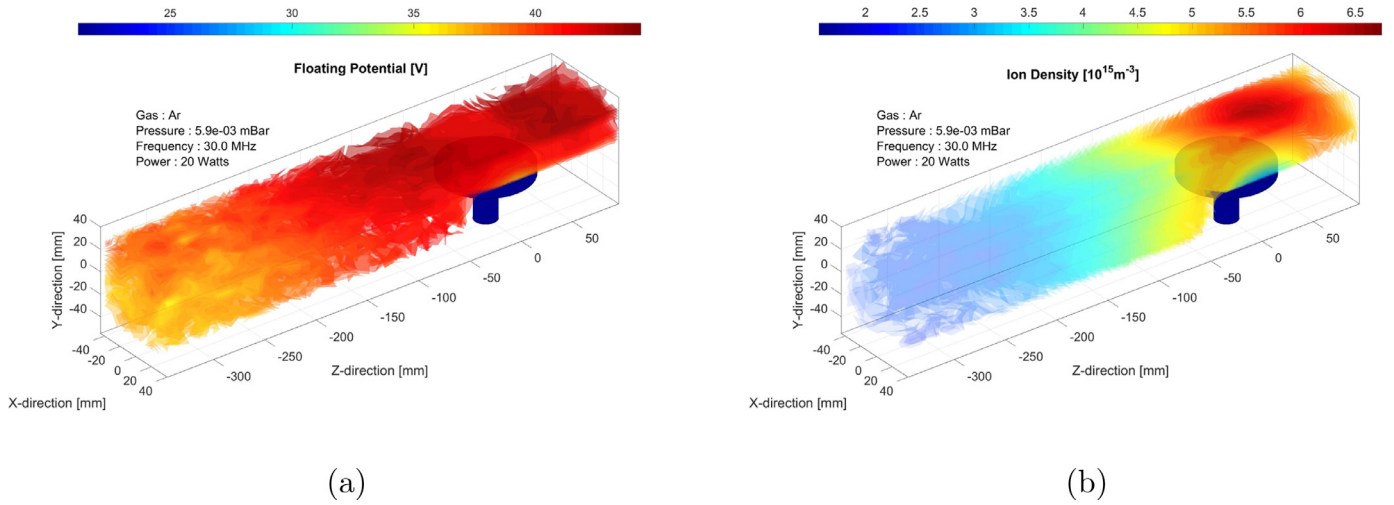


Fig. 2. (a) Floating potential around the RF antenna delivering an input power of 20 W at 30 MHz. The floating potential is uniform over distances of tens of cm. (b) The corresponding ion density peaks in 3D structure visible on top of the antenna. Density slowly decreases along the axis. The sheath is visible as a steep drop of density close to the antenna.

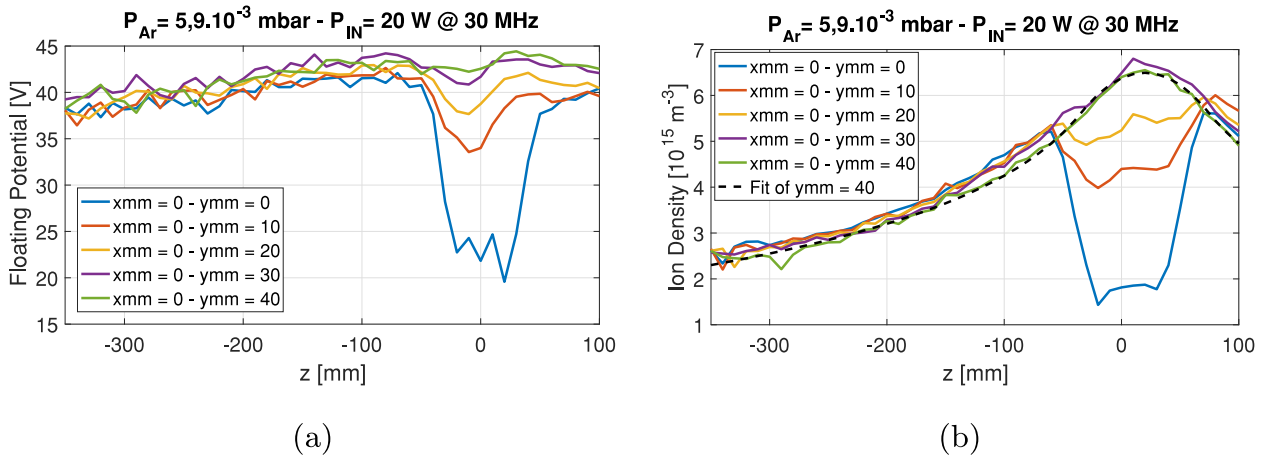


Fig. 3. (a) Floating potential along the z -axis at different elevations (the antenna located between $-40 \text{ mm} < z < 40 \text{ mm}$). The drops of potential observed below $y = 20 \text{ mm}$ correspond to the sheath. (b) Ion density profiles. The density drops in the profiles between $-50 < z < 50$ corresponds to the density depletion within the sheath. Outside this area, the density profiles match the profile given by ambipolar diffusion, as the theoretical dashed black profile confirms.

potential V_{Floating} via the formula [8]

$$T_e = \frac{V_{\text{Plasma}} - V_{\text{Floating}}}{-\frac{1}{2} \ln \left(2\pi \frac{m_e}{m_i} \left(1 + \frac{T_i}{T_e} \right) \right)} \approx \frac{V_{\text{Plasma}} - V_{\text{Floating}}}{4.66} \quad (1)$$

where T_e and T_i are the electron and ion temperature in eV, m_e and m_i are the electron and the ion mass, respectively.

This agreement comforts us in the idea that our data are properly processed for those parameters and allows us to proceed with the analysis. The uniformity of the potential over several tens of centimeters indicates a low resistivity of the plasma. If the potential is rather uniform, this is not the case of ion density map presented on Fig. 2b. Ion density is derived from the ion part of the IV characteristics, taking into account an expansion of the sheath described by the weakly collisional regime described in [9]. On that map one can clearly see a structure above the RF antenna where the ion density peaks at $6.5 \times 10^{15} \text{ m}^{-3}$ whereas the rest of the plasma falls below $4.0 \times 10^{15} \text{ m}^{-3}$ for distances larger than 50 mm away from the antenna. The density keeps falling with the distance and goes down to $1.5 \times 10^{15} \text{ m}^{-3}$ at 350 mm away from the center of antenna. The 3D structure where the ion density peaks is interpreted as the area where the plasma is actually created by the RF antenna, before drifting away in all the directions due to diffusion processes. A closer look at the situation is provided by Fig. 3a

and b, where 1D profiles of the floating potential and the ion density along the z axis are respectively provided. These profiles corresponds to the previous 3D maps for different elevations above the antenna (which lies at $y = -10 \text{ mm}$) and passing through its center at $x = 0 \text{ mm}$. In both figures, green and violet curves correspond to profiles at elevation of 50 mm and 40 mm (of which the surface lies at $y = -10 \text{ mm}$, between $z = -35 \text{ mm}$ and 45 mm) and go through the plasma creation volume. The potential is relatively flat directly on top of the antenna and slowly decreases with distance afterward ($|z| > 40 \text{ mm}$). At the same time, the ion density peaks at $z = 5 \text{ mm}$, roughly above the center of the antenna which is slightly shifted along this direction. The measured profile can very well be reproduced with a fit based on the ambipolar diffusion, assuming a cylindrical symmetry around the axis of the antenna, as in (2).

$$\frac{D_a}{r} \frac{\partial}{\partial r} \left(r \frac{\partial n(r)}{\partial r} \right) = S(r) \quad (2)$$

where D_a is the ambipolar diffusion coefficient, $n(r)$ the density and r the radial coordinate. The source term $S(r)$ is a step function with an adjustable width and height. An example of the success of the fit procedure is provided by the black dashed curve which reproduces the green profile ($y=40 \text{ mm}$). The quality of the fit confirms that plasma is dominated by the modeled am-

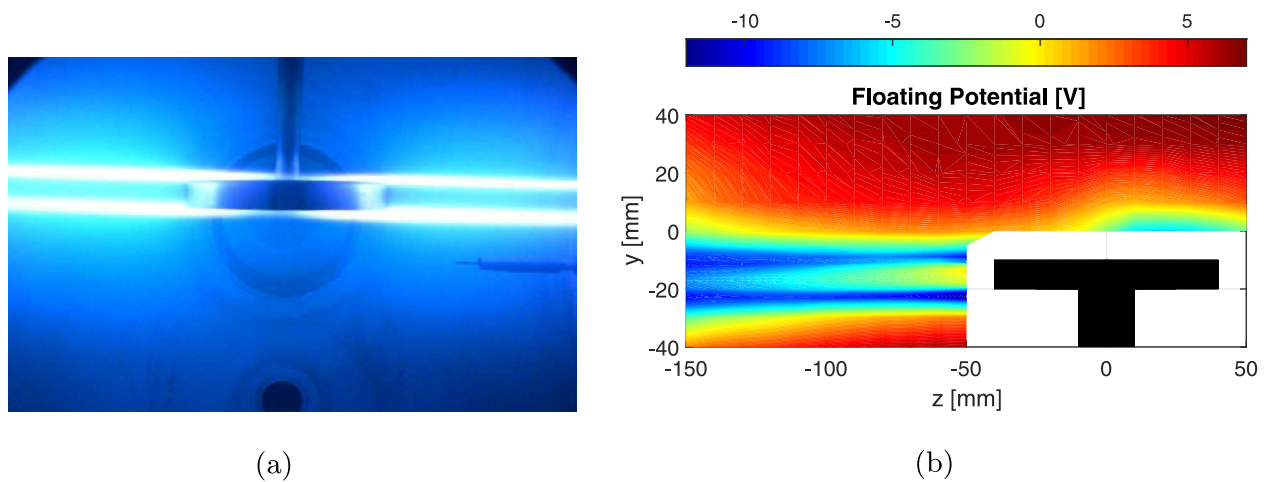


Fig. 4. (a) Visible image of a magnetized plasma in ALINE. Two very bright layers appear on both sides of the antenna. The probe appears on the right part of the picture. $P_{Ar} = 8.9 \times 10^3$ mbar, $P_{RF} = 50$ W, $F = 16.6$ MHz, $B = 0.1$ T (b) 2D map of floating potential around the antenna. Two potential wells extend from both side of the antenna and propagate along the magnetic field lines ($B = 0.05$ T). $P_{RF} = 50$ W at 35.0 MHz and $P_{Ar} = 1.1 \times 10^2$ mbar. (For interpretation of the references to color in this figure legend, the reader is referred to the web version of this article.)

bipolar diffusion. The ambipolar diffusion coefficient obtained from the fit procedure, $D_a^{fit} = 1.28$ m²s⁻¹ is compatible with $D_a^{estimated} = 1.45$ m²s⁻¹ derived from experimental determination of Argon cross-section [10]. This corresponds to an ion mean free path of 2.3 mm, i.e. much smaller than ALINE device. From the modelling, the source area is found to extend up to 54.1 mm from the center, which is in a good agreement with the extent of the sheath observed in both Fig. 3a and b.

The other three curves, on both Fig. 3a and b, display on top of the antenna a large drop in floating potential and ion density, respectively. These depletions are explained by the fact that these profiles pass through the pre-sheath/sheath area, at different depths. In those areas, electron and ion densities are both expected to drop by more than a factor two [11]. Outside the sheath area, the profiles are similar to the ones described before, dominated by ambipolar diffusion.

Maps in a magnetized plasma

We now present 2D maps similar to those described in the previous section, but for a magnetized Argon plasma at $P_{Ar} = 8.9 \times 10^3$ mbar, for $P_{RF} = 50$ W injected at 16.6 MHz. The magnetic field intensity is of 0.1 T. On Fig. 4a an image recorded by a HD webcam is presented. The main striking features are the two very bright layers of light observed on both sides of the antenna. Their blue color is thought to be due to the metastable Ar⁺ ions of the plasma but a spectroscopic analysis would need to confirm it. These two layers are entangled with two lobes of diffuse light, which have an approximatively ellipsoid shape. The two layers are attached on the external surface of the antenna, i.e. above and underneath it, and extend over its full width. They can then be followed (not seen on the picture) all the way down to the vacuum chamber, where they connect to a metallic surface on the probe side (to the right on the picture) and glass window on the other side. For our magnetized plasma, probe measurements of densities are a very delicate question which requires a lot of attention concerning the theory describing the sheath (magnetized electrons and weakly magnetized ions) as well as for the collection area different for the different species. For this reason we only present here a map of floating potential: even if its interpretation remains difficult for the reason mentioned above, its measurement is still straightforward and gives an insight on what happens within the plasma. On Fig. 4b, a bidimensional map of floating potential is shown, for the zOy plane cutting through the middle of the an-

tenna. Two structures similar to the ones observed in the visible image are present. They correspond to values of floating potential around -12 V. This value is considerably lower than its value in the rest of the chamber, where it stays roughly constant at 5 V \pm 2 V. On Fig. 4b, one can see a broadening of the negative floating potential structures with the distance, broadening which occurs in the direction perpendicular to the magnetic lines. Even if we do think that such a process exists, it has to be confirmed by further investigations. The observed phenomenon is likely to be enhanced on the map by the reduction of space resolution of the spatial grid used for measurements.

The origin of these potential wells is likely to be the potential drop within the sheath/pre-sheaths attached to the antenna. The plasma modifications in this area would then propagate along the magnetic lines. This would also explain the negative value of the floating potential, as the self-biasing of the antenna is usually of the order of -100 V (not automatically monitored). Even if a RF compensation problem cannot be fully excluded at that, it is considered unlikely. More reasonable candidates for those drops of potential can be an increase of the electron temperature, the presence of electrons due to secondary emission from the antenna, an increased diffusion of ions across the magnetic lines, a local modification of plasma impedance or all of the above. All these effects will increase the imbalance between ions and electrons and deepen the potential wells. Another interesting question to be investigated is about both the ion and electron density profile in those layers and whether or not a charge imbalance appears, at least in the vicinity of the antenna. A recent publication [12] has investigated by means of numerical simulations the plasma-wall transition for a magnetic field parallel to the wall. It predicts simple laws for quantities such as the sheath size that could be checked. Unfortunately, for magnetized plasmas in ALINE, ion and electron density measurements are not robust enough so far to answer the question, and more work needs to be carried out both experimentally and numerically.

Conclusion and perspectives

In the present paper we have presented the first outputs coming from the ALINE device. The diagnostics now routinely available allow for the measurement of plasma properties in the full space surrounding a RF antenna. The maps of densities and floating potential shown have a spatial accuracy down to 0.1 mm in all directions, which allows for a complete mapping of the chamber, as

well as a detailed investigation of the sheath surrounding the RF antenna. Measurements in unmagnetized plasmas have confirmed that the plasma is mainly created in a 3D structure that extends on top of the RF antenna. The plasma is then driven by ambipolar flow towards the walls of the vessel. In magnetized plasmas, probe measurements are more difficult to interpret. Nonetheless, the two bright layers of plasma observed in the visible picture have been linked to two electric potential wells that develop on both faces of the antenna and propagate along the magnetic field lines. The detailed understanding of this area needs further investigations to be carried out. In the future, a new holder for the antenna will be installed. It will then be possible to vary the angle between its surface and the magnetic field could be varied and its influence be investigated. On top, ALINE is also equipped with a generator delivering electromagnetic waves at the Electron Cyclotron Resonance frequency, i.e. 2.45 GHz, with an input power of 3 kW. This second power source will allow the generation of plasma while using the antenna as a polarizable target to study sheaths around a non-active surface. This capability of ALINE has already been tested but is still under commissioning. This will open the way to experimentally investigate the disappearance of the sheath for grazing incidence of the magnetic field which has been reported both analytically [13] and numerically [14]. The experimental investigations in ALINE will be backed by the continuous development of simulation codes that aims to describe the plasma-wall transition as well as the measurements by Langmuir probes.

Funding

This work was supported by the French National Research Agency through contract no. ANR-12-JS09-0013-01 SPICE RF.

References

- [1] R. Chodura, Plasma-wall transition in an oblique magnetic field, *Phys. Fluids* 25 (1982) 1628, doi:[10.1063/1.863955](https://doi.org/10.1063/1.863955).
- [2] M.A. Lieberman, Analytical solution for capacitive rf sheath, *IEEE Trans. Plasma Sci.* 16 (6) (1988) 638–644, doi:[10.1109/27.16552](https://doi.org/10.1109/27.16552).
- [3] V.A. Godyak, N. Sternberg, Dynamic model of the electrode sheaths in symmetrically driven rf discharges, *Phys. Rev. A* 42 (1990) 2299–2312, doi:[10.1103/PhysRevA.42.2299](https://doi.org/10.1103/PhysRevA.42.2299).
- [4] E. Faudot, S. Devaux, J. Moritz, S. Heuraux, P.M. Cabrera, F. Brochard, A linear radio frequency plasma reactor for potential and current mapping in a magnetized plasma, *Rev. Sci. Instrum.* 86 (6) (2015) 063502, doi:[10.1063/1.4921905](https://doi.org/10.1063/1.4921905).
- [5] I.D. Sudit, F.F. Chen, Rf compensated probes for high-density discharges, *Plasma Sources Sci. Technol.* 3 (2) (1994) 162, doi:[10.1088/0963-0252/3/2/006](https://doi.org/10.1088/0963-0252/3/2/006).
- [6] F.F. Chen, Langmuir probes in rf plasma: surprising validity of oml theory, *Plasma Sources Sci. Technol.* 18 (3) (2009) 035012, doi:[10.1088/0963-0252/18/3/035012](https://doi.org/10.1088/0963-0252/18/3/035012).
- [7] F.F. Chen, J.D. Evans, D. Arnush, A floating potential method for measuring ion density, *Phys. Plasmas* 9 (4) (2002) 1449–1455, doi:[10.1063/1.1462630](https://doi.org/10.1063/1.1462630).
- [8] F. Chen, *Mini-course on plasma diagnostics, IEEE-ICOPS Meeting, Jeju, Korea, 2003*.
- [9] P. Chabert, N. Braithwaite, *Physics of Radio-Frequency Plasmas*, Cambridge University Press, Cambridge, 2011.
- [10] A.V. Phelps, C.H. Greene, J.P.B. Jr, A.V. Phelps, Collision cross sections for argon atoms with argon atoms for energies from 0.01 eV to 10 keV, *J. Phys. B* 33 (16) (2000) 2965, doi:[10.1088/0953-4075/33/16/303](https://doi.org/10.1088/0953-4075/33/16/303).
- [11] S. Devaux, G. Manfredi, Vlasov simulations of plasma-wall interactions in a magnetized and weakly collisional plasma, *Phys. Plasma* 13 (2006) 083504.
- [12] J. Moritz, E. Faudot, S. Devaux, S. Heuraux, Plasma sheath properties in a magnetic field parallel to the wall, *Phys. Plasma* 23 (6) (2016) 062509, doi:[10.1063/1.4953897](https://doi.org/10.1063/1.4953897).
- [13] P. Stangeby, The chodura sheath for angles of a few degrees between the magnetic field and the surface of divertor targets and limiters, *Nuclear Fusion* 52 (2012) 083012, doi:[10.1088/0029-5515/52/8/083012](https://doi.org/10.1088/0029-5515/52/8/083012).
- [14] D. Coulette, G. Manfredi, Kinetic simulations of the chodura and debye sheaths for magnetic fields with grazing incidence, *Plasma Phys. Controlled Fusion* 58 (2) (2016) 025008, doi:[10.1088/0741-3335/58/2/025008](https://doi.org/10.1088/0741-3335/58/2/025008).